Mon. Not. R. Astron. Soc. **000**, 1–7 (2014) Printed 4 March 2014 (MN LATEX style file v2.2)

Geometrically thin acrretion disk around white dwarfs and quark stars

B. Mishra[1⋆], W. Kluźniak[1], B. Vaidya[2]
[1] *Copernicus Astronomical Center, Bartycka 18, Warsaw,00-716, Poland*
[2] *Dipartimento di Fisica 'Amedeo Avogadro' Universit degli Studi di Torino, Via Pietro Giuria 1, 10125 Torino, Italy*

Accepted *** Received 000

ABSTRACT
We have developed a semi-analytic and numerical model to study the geometrically thin and optically thick accretion disk. The central object is a rapidly rotating quark star or white dwarf. We used potential for central object as Maclaurin spheroid potential. The main interest is to investigate the inner region of the so called alpha-disk, alpha being the viscosity parameter. Analytical calculations are mainly done in the radiation pressure dominated region of the accretion disk. Numerical work has been carried out to see the time evolution of the accretion disk around quark stars and white dwarfs using the same potential for Maclaurin spheroids. We found that the change in eccentricity of the compact object gives a minor change in the spectra emitted from the accretion disk. We also found that change in eccentricity of the central object changes the disk thickness, surface density, temperature and radial velocity. In numerical model we showed that if the eccentricity of the object is high the matter will diffuse slowly and advect rapidly during its evolution. This gives a clue that how spin-up or spin-down can change the time evolution of the accretion disk using a very simple Newtonian approach.

Key words: Maclaurin spheroids, white dwarfs, quark stars, accretion disk

1 INTRODUCTION

Accretion disk has remained a challenging problem mainly in the context of its viscosity prescription and radiative processes. The best known models for describing the accretion disk were proposed by Shakura and Sunyaev(1973) (SS73 here after), Novikov and Thorne (1973) and Lynden-Bell and Pringle(1974). The underling assumption behind all these models was a geometrically thin accretion disk because of assumption that accreting gas is cool as compare to the local virial temperature. There was also an assumption of equilibrium between viscous energy generation inside the disk and radiative cooling from the surface of the disk, where radiative cooling was computed with an assumption that disk is optically thick in the vertical direction. Although these models has been intensively used to describe the accretion disk around different accreting sources however these models are more suitable for accreting sources like white dwarfs and neutron stars. These models had less successful implications directly to sources like black holes where gravity is much higher and one has to take into account the consequences of Lightman-Eardley instability.

In the seminal paper SS73 analytically solved the accretion disk model assuming that the source of viscosity is turbulence present in the accretion disk. Till date the exact mechanism of existing viscosity in the accretion disk is not clear. Ballbus Hawley 1991 considered magneto-rotational instability (MRI) to explain the source of viscosity, which fulfills some of the criterion for viscosity in the accretion disk. We shall consider a simple constant α viscosity model to study the accretion disk around quark-stars and white dwarfs without considering effect of magnetic field.

SS73 considered Newtonian potential around spherically symmetric black holes. First time we are considering the accretion disk around an accreting source which has spheroidal shape rather than spherical. We shall use Maclaurin spheroid potential for a constant density and mass of the central accreting object. We investigated that how the non-keplerian angular velocity will change the dynamics of the accreting matter into the source. Our goal is to study mainly inner region of the accretion disk where the multipole effects of chosen Maclaurin spheroid potential dominates. We followed the same model as SS73 just by changing the potential of the central object for Maclaurin spheroid. We used same constant α viscosity prescription to proceed analytic and numerical work. We did the analytical calculation of various parameters of the accretion in all three regions but we

⋆ E-mail: mbhupe@camk.edu.pl

shall focus only in the inner region which is also radiation pressure dominated region as per choice of the SS73 model.

We took into account the main property of the choice of such a potential which corresponds to innermost stable circular orbit (ISCO) even in Newtonian dynamics (Kluzniak et al 13). We chose a constant density and mass quark star and assumed that it is rotating very rapidly. Since during rapid rotation it can change its eccentricity and so semi-major axis of the star. Either eccentricity can decrease or increase, depending on it the semi-major axis will decrease or increase. In Kluzniak et al 13, it has been shown that if the eccentricity is less than a critical value of $e_c = 0.8345$, the ISCO will lie on the equator of the acreting source but if it is higher than this critical value it will be detached from the surface of the star. Keeping this change in ISCO we assumed the cases where eccentricity is less than critical limit. We see a change in inner radii of the accretion disk with change in eccentricity because the semi-major axis of the accreting quark star is changing. This change in the inner radii of the accretion disk due to change in eccentricity will clearly change the calculated parameters like surface density, height and emitted spectra of the accretion disk. However there is very minor change in the steady state results so we also investigated the non-stationary accretion disk.

We studied the time evolution of the accretion disk around quark star by solving the diffusion equation for the matter around accreting source. We again assumed the same potential as in steady disk study. In numerical work we studied that how change in eccentricity will change the time evolution of the accretion disk. We shall describe in the results that higher the eccentricity lower the diffusion of matter and lower the eccentricity higher the diffusion of the matter. In all cases we made a cross check to our results by taking limit that $e \to 0$, this will assure us that our analytical and numerical results are consistent with the existing results.

The article is organized in the following manner. In §2 we described physical model of accretion disk which covers steady thin disk and also numerical study of the time evolution of the accretion disk. §3 is devoted for describing all the results we obtained analytically and numerically. In §4 we shall discuss all the results described in §3 and we shall conclude in §5 with some real future applications of our accretion model around quark stars and white dwarfs.

2 PHYSICAL MODEL

2.1 Maclaurian Spheroid

In general the accretion disk has been studied for the potential due to spherically symmetric objects which corresponds to Keplerian velocity. We are using potential for the Maclaurin spheroids which corresponds to angular velocity which is non-Keplerian in the inner region of the disk. **There is important difference between potential for Maclaurin spheroids and spherical object. The radius R of the Maclaurin spheroid changes with eccentricity and this corresponds to semi-major axis of the star of constant density and mass. We also assumed in our model that the disk inner radius is same as semi-major axis of the central object i.e. disk terminates at the surface of the star. This assumption causes a change in inner radius of the accretion disk due to change in eccentricity of the central body by the following expression.**

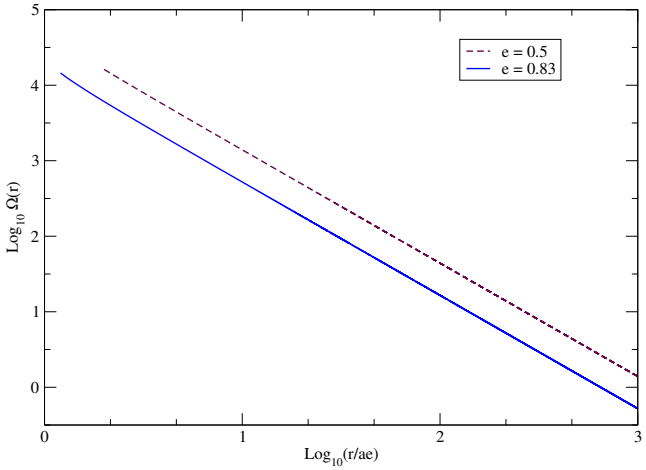

Figure 1. Angular velocity distribution for chosen Maclaurin spheroid potential. The important point to notice in the figure is the inner radii, which varies with eccentricity. This corresponds to different disk inner radii for different values of eccentricity e and corresponding semi-major axis a

$$a = \frac{R}{(1-e^2)^{1/6}} \tag{1}$$

The maximum value of eccentricity in our model is $e = 0.8345$. The reason of this limit is due to fact that in case of potential for Maclaurin spheroids the maximum of radial epicyclic frequency lies at $r = \sqrt{2}ae$ for spheroid eccentricities $e > 1/\sqrt{2}$ but it vanishes for $e_c = 0.83458318$ at the equator of the star (Kluzniak et al 2013). If we still increase the eccentricity further $e > e_c$, the innermost stable circular orbit (ISCO) will be separated from the equator of star and it will be at $r_{ms} = 1.198203ae$ (Kluzniak et al 13). So we always keep the inner radius of the accretion disk at variable semi-major axis of the quark star. One can increase the eccentricity further to investigate the accretion disk for which the inner radii does not lie at the surface of the star but in this model we shall not discuss it. The angular velocity in case of Maclaurin spheroid potential is given by

$$\Omega^2(R) = 2\pi G\rho_* \frac{(1-e^2)^{1/2}}{e^3}\left[\gamma - \cos\gamma \sin\gamma\right] \tag{2}$$

where $\gamma = \arcsin(\frac{ae}{r})$, a is the semi-major axis of the star and ρ_* =const is density of star. Now we have angular velocity of the matter for chosen potential, next goal is to adopt SS73 disk model and redo whole calculations for angular velocity calculated in Eqn. 2.

2.2 Steady thin accretion disk

We considered a geometrically thin accretion disk (height of the accretion disk is much smaller than it's radial structure) to study the steady-state disk around quark-star and white dwarfs. Calculations are done in cylindrical coordinate system (r, ϕ, z), as-

suming azimuthal symmetry. The main interest of this model is to study the steady-state disk to see the behavior of disk parameters and emitted spectra form the accretion disk. To proceed the calculations for steady-state disk we used Eqn. 2 and Eqn. 3 to analytically calculate disk parameters in three different regions (inner region, middle region, outer region) of the accretion disk. In this approach the region of interest is inner region, which is radiation pressure dominated region. In this section we shall present the calculations only for the inner region of the disk in detail . The middle region and outer region are described in the appendix A1. The angular momentum equation in terms of angular velocity is given by

$$\frac{\Sigma d\Omega r^2}{dt} = \frac{1}{r}\frac{d}{dr}W_{r\phi}r^2, \tag{3}$$

where $W_{r\phi}$ is the stress between adjacent layers (SS73), which is defined as function of v_s and surface density Σ.

$$\Sigma = 2\int_0^{z_0} \rho dz, \tag{4}$$

$$W_{r\phi} = -\alpha\Sigma v_s^2, \tag{5}$$

In stationary disk model $\dot{M} = 2\pi\Sigma v_r R =$ const for $v_r < 0$. Now integrating Eqn 3 we obtain

$$\dot{M}\Omega r^2 = -2\pi W_{r\phi}r^2 + C, \tag{6}$$

where C is constant which we calculated by using no-torque boundary condition (SS73). Finally we get the equation to calculate disk parameters in all three regions of the accretion disk.

$$\dot{M}\left(\Omega r^2 - \Omega(a)a^2\right) = 2\pi\alpha\Sigma v_s^2 r^2. \tag{7}$$

Now defining the energy flux radiated from the surface unit as function of Ω is given by

$$Q = -\frac{\dot{M}\left(\Omega r^2 - \Omega(a)a^2\right)}{4\pi r}\frac{d\Omega}{dr}. \tag{8}$$

using Eqn. 7 and Eqn. 8 we calculated disk thickness, surface density, temperature and radial velocity.

2.2.1 Radiation pressure dominated region

SS73 formulated three different regions in the accretion disk, the inner one is radiation pressure dominated where in the interaction of matter and radiation electron scattering on free electrons has dominating contribution. **Fig. 3 verifies our claim that we are studying the inner radiation pressure dominated region**. We shall use Eqn. 7 and Eqn. 8 to obtain the final form of the algebraic equations to calculate the height, surface density, temperature and radial velocity in three different regions of accretion disk (SS73).

$$z_0(r) = \frac{\sigma\rho_0\dot{M}k_1\left(p_1^{1/2}r^2 - p_2^{1/2}R_0^2\right)(ae)^3}{8\pi r^5 c\rho\Omega^2\cos\gamma(\gamma-\sin\gamma\cos\gamma)^{1/2}}. \tag{9}$$

$$\Sigma(r) = \frac{32\pi c^2\rho^2 r^8\cos^2\gamma(\gamma-\sin\gamma\cos\gamma)^2}{\alpha\sigma^2\rho_0^2 k_1^{1/2}(ae)^6\dot{M}\left(p_1^{1/2}r^2 - p_2^{1/2}R_0^2\right)}. \tag{10}$$

$$\varepsilon(r) = \frac{6r^3 c\cos\gamma(\gamma-\sin\gamma\cos\gamma)^{3/2}k_1^{1/2}}{\alpha\sigma(ae)^3} \tag{11}$$

$$T(r) = \frac{6r^3 c\cos\gamma(\gamma-\sin\gamma\cos\gamma)^{3/2}k_1^{1/2}}{b^{1/4}\alpha\sigma(ae)^3} \tag{12}$$

$$\tau(r) = \sqrt{\sigma_T(0.11T^{-7/2}n)}\Sigma(r) \tag{13}$$

$$n(r) = \frac{\Sigma(r)}{2mpz_0(r)} \tag{14}$$

$$v_r(r) = \frac{\dot{M}}{2\pi\Sigma r} \tag{15}$$

where,

$$\gamma = \arcsin(\frac{ae}{r}) \tag{16}$$

$$\gamma_0 = \arcsin(\frac{ae}{R_0}) \tag{17}$$

$$p_1 = (\gamma - \sin\gamma\cos\gamma) \tag{18}$$

$$p_2 = (\gamma_0 - \sin\gamma_0\cos\gamma_0) \tag{19}$$

$\dot{M}$ is mass accretion rate, $z_0(r)$ is half thickness of the disk, $\Sigma(r)$ is the radial distribution of surface density, $\varepsilon(r)$ is radial distribution of energy density, $T(r)$ is radial distribution of the temperature, $\tau(r)$ is optical thickness, $n(r)$ is the number density and v_r is the radial velocity of the matter in the steady thin accretion disk.

2.3 Non-stationary accretion disk

In this model we numerically studied the time evolution of the thin accretion disk around quark stars. The viscosity mechanism causes a transport of angular momentum outwards and matter accretion inwards. This transport of angular momentum is clearly seen in our numerical model. We numerically integrated the diffusion equation Eqn. 20 with constant viscosity ν. We used Crank-Nicolson method which is described in Brensteil et al 2010 to solve the linear diffusion-advection equation. One can also solve the same equation using Green's function but the expressions in case of Maclaurin spheroid potential are not trivial to handle analytically. For the potential we adapted from Maclaurin spheroids gives the different angular velocity profile so we shall write the diffusion equation in terms of angular velocity. The equations we used in our model can be fed with any form of potential or angular velocity to see the time evolution of the accretion disk.

$$\frac{\partial\Sigma}{\partial t} = -\frac{1}{r}\frac{\partial}{\partial r}\left[\frac{1}{2\pi(r^2\Omega)'}\frac{\partial G}{\partial r}\right] \tag{20}$$

$$v_r = \frac{1}{2\pi}\frac{\frac{\partial G}{\partial r}}{r\Sigma(r^2\Omega)'} \tag{21}$$

where,

$$G(r,t) = 2\pi r\nu\Sigma r^2\Omega' \tag{22}$$

is the torque exerted by the outer ring to inner ring in the accretion disk or $-G(r,t)$ is torque exerted by the inner ring to the outer ring. Now if we choose the Keplerian angular velocity the above equations will reduce to diffusion equation used for study of disk evolution by various models based on alpha-disk models.

$$\frac{\partial\Sigma}{\partial t} = \frac{3}{r}\frac{\partial}{\partial r}\left[r^{1/2}\frac{\partial}{\partial r}\left(\nu\Sigma r^{1/2}\right)\right] \tag{23}$$

$$v_r = -\frac{3}{\Sigma r^{1/2}} \frac{\partial}{\partial r} \left(\nu \Sigma r^{1/2}\right) \tag{24}$$

where Σ is the surface density, ν is kinematic viscosity. Now using Eqn. 2, Eqn. 20 and Eqn. 21 we shall compute the time evolution of the accretion disk for different eccentricities e of the quark star. Depending on eccentricity e, either matter can be diffused rapidly or slowly. If the eccentricity is high matter will diffuse very slowly as compare to low eccentricity (inverse law), which we shall describe in the results.

3 RESULTS

3.1 Steady state disk

In this section we shall use Eqn.2 to Eqn.8 to investigate the results in inner (radiation pressure dominated) region of the accretion disk. In this plot we keep accretion rate fixed at $\dot{M} = 10^{14} g/s$ and changed the eccentricity e of the central object to see the effect on the disk thickness, surface density, temperature and radial velocity of accreting matter in the inner region. Fig. 2 shows the variation of the half-thickness $z_0(r)$, surface density $\Sigma(r)$, temperature $T(r)$ and radial velocity $v_r(r)$. In Fig. 2 the inner grid point of the plot for all the parameters is $2a$ to avoid singularities at the inner boundary of the disk. We see from upper left panel of Fig. 2 a difference in the half thickness of the accretion disk for different eccentricities $e = 0.1$, $e = 0.2$ and $e = 0.8345$. Higher eccentricity e of the star corresponds to higher disk thickness at a particular radial distance from the center of star. This is direct consequence of the angular velocity distribution (Fig. 1) due to Maclaurin spheroid potential (Eqn. 2). The half-thickness $z_0(r)$ of accretion disk increases rapidly in the smaller radius but at large radius the disk thickness is almost constant. We see that the thickness of the accretion disk in our steady state model is of the order of few $100cm$, which is very thin disk. The reason of having such a thin disk is directly related to our choice of very low accretion rate of $10^{14} g/s$.

The right panel in Fig. 2 shows the logarithmic plot of the surface density distribution in the inner region of the accretion disk. We see that for higher eccentricities the surface density is higher than for the lower eccentricities. The surface density of steady thin disk in our model varies from about $10^7 g/cm^2$ at the inner boundary to about $10^1 1 g/cm^2$ at the outer boundary of our interest. The surface density $\Sigma(r)$ also increases with radial distance in the inner region of the accretion disk. The lower left panel in Fig. 2 shows the radial variation of temperature $T(r)$ in the accretion disk. We see that for higher eccentricities the temperature is lower. This is due to low angular velocity of the accreting matter for higher values of eccentricities e. A low angular velocity of matter will exert less torque between neighboring rings of the matter in the accretion disk and hence less friction and low temperature. The radial profile of temperature also shows that at large radii the temperature is lower as compare to lower

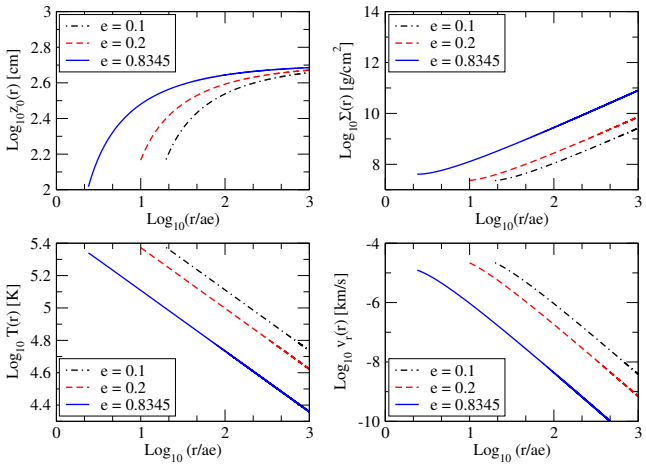

Figure 2. Multiplot of height $z_0(r)$, surface density $\Sigma(r)$, temperature $T(r)$ and radial velocity $v_r(r)$ variation with radial distance from the center of the star

radii. This is again due to angular velocity distribution in the accretion disk. The right lower panel in Fig. 2 shows the radial velocity profile $v_r(r)$ in the accretion disk. The higher eccentricity corresponds to lower radial velocity which is also clear from right upper panel of Fig. 2 where we have higher surface density $\Sigma(r)$ for higher eccentricities e. The radial velocity in our model is of the order of 10^{-5} to 10^{-10} which is low enough to assume that our thin disk model is steady accretion disk.

3.2 Disk thermodynamics and Spectra

The most important parameter for observational interest is emitted spectra from the accretion disk. Emitted spectra corresponds to the size of accretion disk. Fig. 4 shows the emitted spectra from the accretion disk of different size or area. Since the computed spectra is independent of any specified region, we can choose an arbitrary outer radii of the accretion disk to see the behavior of the emitted spectra. Here accretion disk we assumed is optically very thick in the z direction therefore we can assume that each element of the disk emits as black body with temperature $T(r)$. Using angular velocity from Eqn. 2 and equating the dissipation rate per unit area to the black body flux we computed temperature of the accretion disk. Using the calculated temperature we can calculate intensity and with intensity flux of emitted spectra from the accretion disk.

$$T(r) = \left[\frac{-\Omega \frac{d\Omega}{dr} T_1}{4\pi\sigma}\right]^{1/4} \tag{25}$$

where T_1 is defined as

$$T_1 = 1 - \frac{\Omega(a)a^2}{\Omega(r)r^2} \tag{26}$$

Now using a very crude approximation we can approximate the emitted spectra in cgs units by

$$I(\nu) = B_\nu[T(r)] = \frac{2h\nu^3}{c^2(e^{h\nu/kT(r)} - 1)} \tag{27}$$

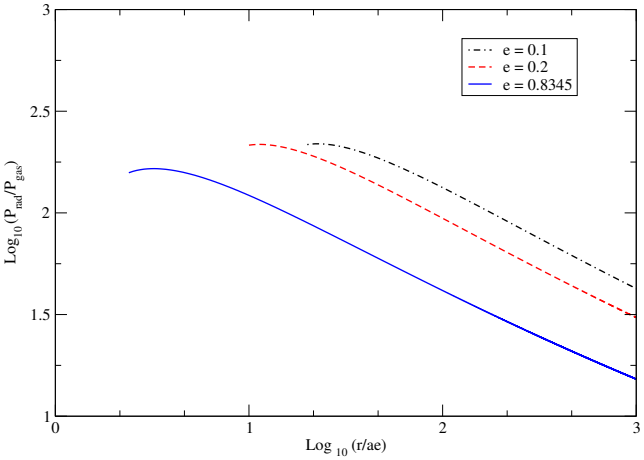

Figure 3. Plot shows the the inner region of investigation in which we assumed that radiation pressure dominates over gas pressure. The vertical axis shows the log of ratio of radiation pressure P_{rad} to gas pressure P_{gas}. The horizontal axis corresponds to scaled radial distance from the center of the star.

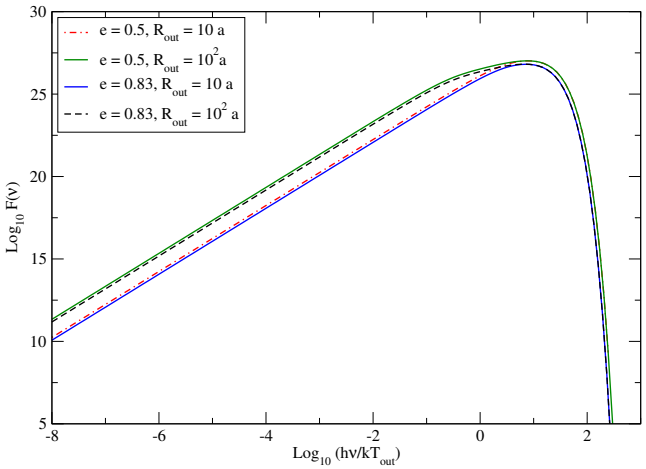

Figure 4. Plot shows the emitted spectra from the accretion disk. The vertical axis shows the log of flux emitted and horizontal axis corresponds to frequency scaled by temperature at outer radius of accretion disk. There is a minor change in spectra emitted due to change in eccentricity of central object.

using Eqn. 26 we computed flux emitted from accretion disk by integrating over the whole disk.

$$F(\nu) = \frac{2\pi}{D^2}\int_{R_{in}}^{R_{out}} I(\nu) r dr \tag{28}$$

the integration of Eqn. 28 gives emitted spectra from the disk (Fig. 4). We chose outer radius of the accretion disk $R_{out} = 10a$ and $R_{out} = 100a$ in Fig. 4 to see the behavior of the emitted spectra for different eccentricity of the quark star. We see clearly that a change in outer radius R_{out} of the disk changes the emitted spectra at lower frequency while change in eccentricity which corresponds to change in inner radii R_{in} of the accretion disk causes a very minor change in emitted spectra at high frequency. There is also a very minor difference across the whole range of the emitted spectra for different eccentricities. At $h\nu/kT = 10$ curves for $e = 0.83$, $R_{out} = 100a$ and $e = 0.5$, $R_{out} = 10a$ have the same value of emitted flux.

3.3 Evolution of surface density

We used the physical model of non-stationary accretion disk described in §2.3 to study the time evolution of accretion disk. We numerically solved Eqn. 20 and Eqn. 21 to study the time evolution of the surface density $\Sigma(r)$. We see from Fig. 2 that for higher values of the eccentricity of accreting quark stars the angular velocity $\omega(r)$ is lower. This also corresponds that if the eccentricity is higher there will be less friction between neighboring rings of the matter in the accretion disk and this will imply slow angular momentum transport outwards and low diffusion of the matter into the accreting source. We considered a Gaussian ring of matter at a radial distance of $r/a = 1.5$ as the initial condition to solve the diffusion equation Eqn. 20. In all the results of non-stationary disk the time is in viscous time scale, $t_{visc} = r^2/\nu$ and the kinematic viscosity coefficient is constant, $\nu = 0.01$. In Fig. 5 we plotted the time evolution of surface density $\Sigma(r)$ scaled with initial surface density of the ring we considered. The horizontal axis corresponds to radial distance

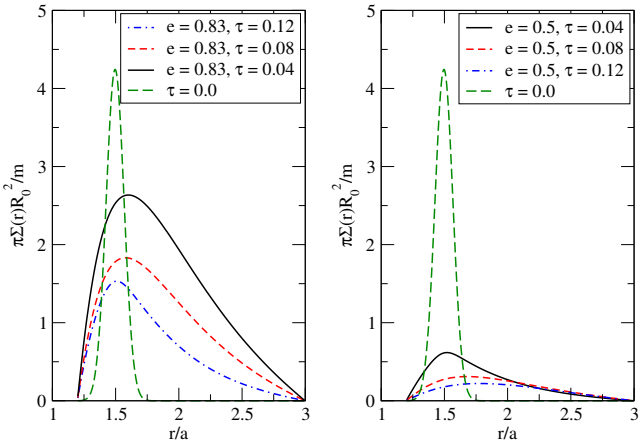

Figure 5. Time evolution of the ring of matter at a radial distance of $r = 1.5ae$. The vertical axis shows the surface density scaled with initial surface density. The horizontal axis corresponds to radial distance form the center of star. We see a inverse law of diffusion and eccentricity.

scaled with semi-major axis of the quark-star. Left panel in Fig. 5 shows the time evolution of the accretion disk for an accreting source with eccentricity $e = 0.83$ and the right panel of Fig. 5 shows the time evolution for eccentricity $e = 0.5$. From Fig. 5 we see that for higher eccentricities the matter has slow diffusion (i.e. diffusion has inverse law with eccentricities).

Fig. 6 shows the time evolution of the ring of matter we put for very low values of eccentricities. Left panel in Fig. 6 shows the time evolution of the ring of matter for eccentricity $e = 0.0001$ and the right panel again same as right panel of Fig. 5 for eccentricity $e = 0.5$. From Fig. 5 and Fig. 6 we can conclude that higher eccentricity of accreting source can slow the accretion process and low eccentricity of accreting source can push the matter much easily into the accreting source like black holes discussed in Lynden-Bell and Pringle (1974).

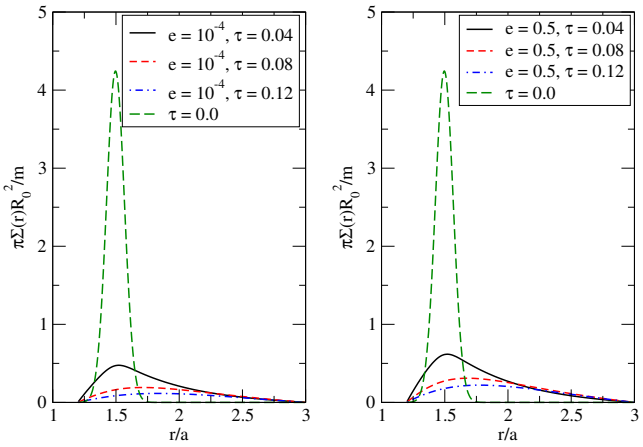

Figure 6. Time evolution of the accretion disk. This plot has same meaning as Fig. 5 but for left panel for a low eccentricity case

4 DISCUSSION

4.1 Very thin and fast disk

- Why few cm sized disk ?
- Is Newtonian gravity responsible for faster disk.
- how values change with change in α.

4.2 Dependence of Spectra on eccentricity

- Explain the reason for the dependence of spectra on e.
- Discuss its consequences in observations.

4.3 Angular Momentum transport in disks

- Explain the reason for skewness in sigma plot with high e values. Show plots of advection and diffusion.
- Also discuss the implication of e on Ang. momentum transport.

5 CONCLUSION

State your conclusions here.

APPENDIX A:

A1 Steady-state disk

A1.1 Gas pressure dominated region, electron scattering

This is the middle region of the accretion disk in which gas pressure dominates over the radiation pressure ($P_g >> P_r$). In this region also similar to inner region electron scattering gives main contribution to opacity. The sound speed in this region is given by $v_s^2 = \frac{kT}{m_p}$.

$$\Sigma(r) = \left(\frac{\dot{M}}{\pi}\right)^{3/5} \left(\frac{m_p}{\alpha k}\right)^{4/5} \left(\frac{bc}{3\sigma}\right)^{1/5} r^{-7/5} \left(\Omega r^2 - \Omega_0 R_0^2\right)^{3/5} \left(\frac{d\Omega}{dr}\right)^{-1/5} \tag{A1}$$

$$T(r) = 0.707106\pi^{-3/20} \left(\frac{3\sigma}{bc}\right)^{1/5} \dot{M}^{2/5} r^{-7/20} \left(\Omega r^2 - \Omega(R_0)R_0^2\right)^{2/5} \left(\frac{m_p}{\alpha k}\frac{d\Omega}{dr}\right)^{1/5} \tag{A2}$$

$$z_0(r) = \sqrt{\frac{kT}{m_p\Omega^2}} \tag{A3}$$

$$n(r) = \frac{\Sigma(r)}{2m_p z_0} \tag{A4}$$

$$\tau(r) = \sqrt{\sigma_T \sigma_{ff}}\Sigma \tag{A5}$$

$$v_r = \frac{\dot{M}}{2\pi\Sigma(r)r} \tag{A6}$$

where, Ω is given by Eqn.1, $\Sigma(r)$ is the height integrated surface density, $T(r)$ is the temperature, $z_0(r)$ is the half thickness of the disk, $n(r)$ is the number density, $\tau(r)$ is the optical thickness and v_r is the radial velocity. Ω is the angular velocity, σ is opacity, c is speed of light, α is angular momentum transportation factor, m_p is the mass of proton, σ_T is Thompson cross-section and σ_{ff} is opacity due to free free absorption.

A1.2 Gas pressure dominated region, free-free absorption

In this region similar to gas pressure dominated region $P_g > P_r$ but the opacity is determined by free-free absorption. Sound speed is defined similar to middle region (gas pressure dominated region with electron scattering) $v_s^2 = \frac{kT}{m_p}$.

$$\Sigma(r) = \left(\frac{m_p}{(2\pi\alpha k)^{4/5}}\right) \left(\frac{32\pi Rbc\dot{M}^7 \left(\Omega r^2 - \Omega_0 R_0^2\right)}{3\Omega\frac{d\Omega}{dr}}\right)^{1/10} \tag{A7}$$

$$T(r) = \left(\frac{3Q\Sigma^{1/2}\Omega}{2m_p^{1/2}}\right)^{1/8} \tag{A8}$$

$$z_0(r) = \sqrt{\frac{kT(r)}{m_p\Omega^2}} \tag{A9}$$

$$n(r) = \frac{\Sigma(r)}{2m_p z_0(r)} \tag{A10}$$

$$\tau = \sigma_{ff}\Sigma(r) \tag{A11}$$

$$v_r = \frac{\dot{M}}{2\pi\Sigma(r)r} \tag{A12}$$

where

$$Q = -\frac{\dot{M}\left(\Omega r^2 - \Omega(R_0)R_0^2\right)}{4\pi r}\frac{d\Omega}{dr}. \tag{A13}$$

is the energy flux radiated from unit surface of disk in unit time and rest of the parameters defined above have the same notation as in the inner region and middle region of the accretion disk.

A2 Non-stationary accretion disk

The Crank-Nicolson algorithm we used has been already described in very detail for solving a general form of advection-diffusion equation (Brinsteil et al 2010). Here we shall describe the different terms which we calculated for our model to fit with Eqn. A14

$$\frac{\partial \Sigma}{\partial t} + \frac{\partial}{\partial x}(\Sigma u) - \frac{\partial}{\partial}\left[hD\frac{\partial}{\partial x}\left(\nu\frac{\Sigma}{h}\right)\right] = L\Sigma \tag{A14}$$

where

$$D = \frac{r\Omega'}{(2\Omega + r\Omega')} \tag{A15}$$

$$u = \frac{\nu\Omega'}{(2\Omega + r\Omega')} \tag{A16}$$

$$h = \frac{1}{r^3\Omega'} \tag{A17}$$

$$L = -\nu r^3\Omega'\left[\frac{3}{r^4 l_1} + \frac{3\Omega' + r\Omega''}{r^3 l_1^2}\right] \tag{A18}$$

where again,

$$l1 = (2\Omega + r\Omega') \tag{A19}$$